



A new numerical algorithm based on Quintic B-Spline and adaptive time integrator for Coupled Burger's equation

Yesim Çiçek¹, Nurcan Gucuyenen Kaymak^{2,*}, Ersin Bahar³, Gurhan Gurarlan³, and Gamze Tanoğlu⁴

¹Engineering Sciences, Faculty of Architecture and Engineering, Izmir Katip Çelebi University, Izmir, Turkey.

²Management Information Systems, Faculty of Economics and Administrative Sciences, Doğuş University, Istanbul, Turkey.

³ Department of Civil Engineering, Pamukkale University, Denizli, Turkey.

⁴Department of Mathematics, Izmir Institute of Technology, Izmir, Turkey.

Abstract

In this article, the coupled Burger's equation which is one of the known systems of the nonlinear parabolic partial differential equations is studied. The method presented here is based on a combination of the quintic B-spline and a high order time integration scheme known as adaptive Runge-Kutta method. First of all, the application of the new algorithm on the coupled Burger's equation is presented. Then, the convergence of the algorithm is studied in a theorem. Finally, to test the efficiency of the new method, coupled Burger's equations in literature are studied. We observed that the presented method has better accuracy and efficiency compared to the other methods in the literature.

Keywords. Quintic B-Spline, Adaptive Runge-Kutta method, Coupled Burger's equation, Non-linear parabolic partial differential equation.

2010 Mathematics Subject Classification. 65L05, 34K06, 34K28.

1. INTRODUCTION

Formulation of a wide range of mathematical and engineering problems leads to nonlinear partial differential equations. Being a coupled partial differential equation, Burger's equations describe the approximation theory of flow through a shock wave that travels in a viscous fluid [1].

Recently, many authors have studied various types of coupled Burger's equations by using different numerical and approximation methods. In 2009, Rashid and Ismail applied Fourier pseudospectral approach to one-dimensional coupled Burger's equation [19]. The collocation-based numerical scheme is applied to coupled Burger's equation in [16]. The radial basis function (RBF) collocation method has been formulated and the mesh-free method is applied for the numerical solution of coupled Burger's equations and other nonlinear PDEs [9]. The Chebyshev spectral collocation method was developed using Chebyshev polynomials, and the Runge-Kutta 4th order method (RK4) is applied in [11]. Coupled viscous Burger's equations are studied by Mittal and Arora using cubic B-spline collocation scheme in [14]. Rashid et al. studied coupled viscous Burger's equation by using Chebyshev–Legendre pseudospectral method where the leapfrog scheme is applied for time direction in [20]. A composite numerical technique which is obtained by Haar wavelets and finite difference methods is used to obtain the numerical solution of the coupled Burger's equation by Kumar and Pandit in [13]. In [21], an improved backward substitution method is applied to time-dependent nonlinear coupled Burger's equations. Also, in 2019, a semi-Lagrangian approach was used for the numerical solution of coupled Burger's equations, [3]. It is clear that various methods have been applied to the coupled Burger's equation, but more works such as convergence analysis and efficient numerical schemes are encouraged for different parameters.

Methods based on B-spline functions have attracted great interest in recent years due to their simple implementations and effective solutions by researchers. Quartic and quintic B-spline methods are applied for the space derivatives

Received: 01 April 2022 ; Accepted: 15 June 2022.

* Corresponding author. Email: nkaymak@dogus.edu.tr .

in [12]. With the help of this approximation on the given partial derivatives, the system of partial differential equations can be transformed into ordinary differential equations. In [17], a cubic trigonometric B-spline with a collocation method is used to solve one-dimensional convection-diffusion problems. Cubic and quintic B-spline collocation methods are applied and combined with the Crank-Nicolson scheme for time integration in [8] and [18]. It can be seen that many different types of B-spline methods are preferred to use for the solution of different kinds of partial differential equations. Still, the combination with the adaptive time method has a great effect on accuracy. In [2], an approximation method based on B-spline bases and the method of lines approach is exhibited for advection-diffusion equations. It is the actual work that inspired the creation of this work.

In the presented paper, a new algorithm is constructed by combining quintic B-spline in space and a fifth-order Runge-Kutta method in time for the following coupled Burger’s equation, see [14–16]:

$$u_t = u_{xx} - \eta uu_x - p(uv)_x, \quad a \leq x \leq b, \quad 0 \leq t \leq T, \tag{1.1}$$

$$v_t = v_{xx} - \xi vv_x - q(uv)_x, \quad a \leq x \leq b, \quad 0 \leq t \leq T, \tag{1.2}$$

where η, p, ξ and q are some constants which depend on the Stokes velocity with the following initial and boundary conditions,

$$u(x, 0) = f_1(x), \quad v(x, 0) = f_2(x), \quad a < x < b, \tag{1.3}$$

$$u(a, t) = g_1(t), \quad u(b, t) = g_2(t), \quad 0 \leq t < T, \tag{1.4}$$

$$v(a, t) = g_3(t), \quad v(b, t) = g_4(t), \quad 0 \leq t < T. \tag{1.5}$$

The convergence of the new algorithm is proved in Theorem 3.1. To present the efficiency of the proposed method, coupled Burger’s equations are studied with three different initial and boundary conditions, see [14–16]. The results are presented with various tables and graphics.

These are the motivations of this paper: First of all, the proposed method is easy to implement for nonlinear parabolic partial differential equations. Secondly, when compared to other methods in the literature,[16], the proposed method gives more accurate results and smaller errors in both L_2 and L_∞ norms for various final times. What is more, computed results are in good agreement with the literature [14, 15]. Finally, the numerical solutions can be computed in less than four seconds CPU times for the third example.

The study has been organized as follows: In section 2, a brief description of the presented technique in both space and time. The convergence of the new algorithm is proved in Theorem 3.1, in section 3. Section 4 is dedicated to presenting several examples to highlight the efficiency and accuracy of the presented scheme by comparing it to the other methods in the literature. Finally, we conclude the study in section 5.

2. APPLICATION OF THE METHOD

In this part, application of the proposed method on coupled Burger’s equations (1.1)-(1.2) is studied. Firstly, in space discretization, the way of use of quintic B-spline method is introduced with the help of coefficients given in Table 1. After embedding quintic B-spline equivalence of each term in Eqs.(1.1)-(1.2), the system of coupled Burger’s equations turns into a system of ordinary differential equations given in (2.15). Later, DOPRI5, [6], is used in time discretization with the help of Butcher table in Table 2.

2.1. Quintic B-spline collocation method. Let solution domain $[a, b]$ be divided into a uniform mesh of length $h = x_{j+1} - x_j$ by nodes x_j where $j = 0, 1, \dots, N$.

The exact solutions to Eqs. (1.1)-(1.2) can be approximated by $U(x, t), V(x, t)$, respectively. Then, they can be written in the following form

$$u(x, t) \approx U(x, t) = \sum_{j=-2}^{N+2} c_j(t)B_j(x), \tag{2.1}$$



$$c^0 = \begin{pmatrix} c_0^0 \\ c_1^0 \\ \vdots \\ c_{N-1}^0 \\ c_N^0 \end{pmatrix}, d^0 = \begin{pmatrix} d_0^0 \\ d_1^0 \\ \vdots \\ d_{N-1}^0 \\ d_N^0 \end{pmatrix},$$

and

$$R_1 = \begin{pmatrix} f_1(x_0) + \frac{3h}{5}l_1 + \frac{h^2}{10}l_3 \\ f_1(x_1) + \frac{h}{40}l_1 + \frac{h^2}{160}l_3 \\ f_1(x_2) \\ \vdots \\ f_1(x_{N-1}) \\ f_1(x_N) - \frac{h}{40}l_2 + \frac{h^2}{1600}l_4 \\ f_1(x_{N+1}) - \frac{3h}{5}l_2 + \frac{h^2}{10}l_4 \end{pmatrix} R_2 = \begin{pmatrix} f_2(a) + \frac{3h}{5}m_1 + \frac{h^2}{10}m_3 \\ f_2(x_1) + \frac{h}{40}m_1 + \frac{h^2}{160}m_3 \\ f_2(x_2) \\ \vdots \\ f_2(x_{N-1}) \\ f_2(x_N) - \frac{h}{40}m_2 + \frac{h^2}{1600}m_4 \\ f_2(x_{N+1}) - \frac{3h}{5}m_2 + \frac{h^2}{10}m_4 \end{pmatrix},$$

with space nodes $x_j = a + j * h, j = 0, 1, \dots, N - 1, N$ $h = (b - a)/N$ and $l_1(0) = l_1, l_2(0) = l_2, l_3(0) = l_3, l_4(0) = l_4, m_1(0) = m_1, m_2(0) = m_2, m_3(0) = m_3, m_4(0) = m_4.$

Consequently, first and second derivative matrices can be found by Eqs. (2.4-2.5) and (2.7-2.8), respectively since the parameter matrices are known.

For the sake of simplicity in the coupled Burger’s Eqs.(1.1)-(1.2), we define $W = (u, v)^T$ and then have

$$W_t(x, t) = AW(x, t) + f(t, W), \tag{2.15}$$

$$W(x, t_0) = W_0(x), \tag{2.16}$$

where $A = \begin{pmatrix} \partial x^2 & 0 \\ 0 & \partial x^2 \end{pmatrix}, f(t, W) = \begin{pmatrix} 2uu_x - uv_x - u_xv \\ 2vv_x - uv_x - u_xv \end{pmatrix},$

$$W(x, t_0) = [f_1(t_0), f_2(t_0)]^T.$$

When the spatial derivatives in Eq. (2.15) are discretized by QBS functions, the following time-dependent nonlinear ordinary differential equation system is obtained:

$$\tilde{W}_t = \tilde{A}\tilde{W} + \tilde{f}(t, \tilde{W}). \tag{2.17}$$

Here, \tilde{W} is a $2(N + 1) \times 1$ size vector and \tilde{A} is spatial discretization matrix with $2(N + 1) \times 2(N + 1)$ size and $\tilde{f}(t, \tilde{W})$ is nonlinear part with size of $2(N + 1) \times 1$ where N is the number of discretization points in x-direction.

2.3. Time discretization. In this section, a fifth order adaptive Runge-Kutta method, DOPRI5, is applied to Eq.(2.17), [5, 6]. Due to the advantages of DOPRI5, being a higher order, reliable, accurate method, and presenting efficient error results, this method has been proposed to solve given coupled Burger’s equations numerically. Eq.(2.17) can be rewritten as:

$$\tilde{W}_t(t) = F(t, \tilde{W}), \tag{2.18}$$

$$\tilde{W}(t_0) = \tilde{W}_0. \tag{2.19}$$



Consider Eq.(2.18), DOPRI5 solution can be obtained as:

$$k_1 = F(t_n, \tilde{W}_n), \tag{2.20}$$

$$k_s = F(t_n + c_s \Delta t_n, \tilde{W}_n + \Delta t_n \sum_{i=1}^{s-1} \psi_{s,i} k_i), \tag{2.21}$$

$$\tilde{W}_{n+1} = \tilde{W}_n + \Delta t_n \sum_{s=1}^7 \Phi_s k_s, \tag{2.22}$$

where n and s denote the time stage index numbers k_s stands for the approximated slope matrix and Δt_n is the adapted time step at $t = t_n$. The coefficients c_s , $\psi_{s,i}$ and Φ_s are obtained by Butcher table, Table 2.

The truncation error for DOPRI5 is obtained by using (2.23). The tolerance error defined by e_{Tol} can be chosen by the user. For a fixed time step $t = t_n$, the error is controlled with condition $\|e_n\| \leq e_{Tol}$. What is more, if ratio $\gamma = \frac{\Delta t_{n+1}}{\Delta t_n}$ is given, we have $\gamma = 0.9(\frac{e_{Tol}}{\|e_{n+1}\|})^{1/5}$. In this study γ is limited to $[0.1, 10]$ and error tolerance is chosen $e_{Tol} = 10^{-6}$.

$$e_{n+1} = \Delta t_n \sum_{s=1}^7 (\Phi_s - \tilde{\Phi}_s) k_s. \tag{2.23}$$

TABLE 2. Butcher Table of DOPRI5

c	ψ						
0	0						
$\frac{1}{3}$	$\frac{1}{3}$	0					
$\frac{2}{3}$	$\frac{2}{3}$	$\frac{9}{32}$	0				
$\frac{1}{10}$	$\frac{40}{44}$	$-\frac{40}{56}$	$\frac{32}{9}$	0			
$\frac{3}{8}$	$\frac{45}{19372}$	$-\frac{15}{25360}$	$\frac{9}{64448}$	$-\frac{212}{729}$	0		
9	$\frac{6561}{9017}$	$-\frac{2187}{355}$	$\frac{6561}{46732}$	$\frac{729}{49}$	$-\frac{5103}{18656}$	0	
1	$\frac{3168}{35}$	0	$\frac{5247}{500}$	$\frac{176}{125}$	$-\frac{2187}{6784}$	$\frac{11}{84}$	0
1	$\frac{384}{35}$	0	$\frac{1113}{500}$	$\frac{192}{125}$	$-\frac{6784}{2187}$	$\frac{84}{11}$	0
Φ^T	384	0	1113	192	6784	84	0
$\tilde{\Phi}^T$	5179	0	7571	393	-92097	187	$\frac{1}{40}$
	57600		166954	640	339200	2100	$\frac{1}{40}$

3. CONVERGENCE RESULTS

The present section aims to analyze the convergence of the presented scheme. For this purpose the following assumptions will be satisfied for Eq. (2.17). For the adaptive Runge-Kutta method, we will use a similar approach to [4] which is based on the analysis of the incoherence between the local and global order reduction for nonlinear systems.

Let \tilde{w}_n approximates the exact solution \tilde{W} of Eq. (2.17) at $t = t_n$ and assume that for a constant matrix \tilde{A} and the vector function \tilde{f} the following inequalities are satisfied

$$\langle \tilde{A}\tilde{w}, \tilde{w} \rangle \leq \beta \|\tilde{w}\|^2, \tag{3.1}$$

$$\langle \tilde{f}(t, \tilde{w}) - \tilde{f}(t, \tilde{u}) \rangle \leq \alpha \|\tilde{w} - \tilde{u}\|, \tag{3.2}$$

for the inner product $\langle ., . \rangle$ defined in $\mathbf{R}^{2(N+1)}$.



We can rewrite DOPRI5 method which is defined by Eqs. (2.20)-(2.22) as follows

$$\tilde{w}_{n+1} = \tilde{w}_n + \Delta t_n \sum_{s=1}^7 \Phi_s F(t_n + c_s \Delta t_n, y_s^n), \tag{3.3}$$

$$y_s^n = \tilde{w}_n + \Delta t_n \sum_{i=1}^{s-1} \Psi_s F(t_n + c_i \Delta t_n, y_i^n), \tag{3.4}$$

where Δt_n is the adapted time step at $t = t_n$ and \tilde{w}_n approximates the exact solution of $\tilde{W}(t)$ at $t = t_n$.

Let Δt_N be constant and $\varepsilon_N = \tilde{W}(t_N) - \tilde{w}_N$, which is the global error at $t = T = N\Delta t$, we can define a bound for ε_N of the following form,

$$\|\varepsilon_N\| \leq C\Delta t_N^p, \quad \Delta t_N \in (0, \Delta \bar{t}_N), \tag{3.5}$$

where $\Delta \bar{t}_N$ is a step size bound and p is the minimal order of all stage of DOPRI5 scheme.

In the following subsection, we analyze the discrepancy between the local and global order reduction in a similar way to [4].

3.1. Recursion Scheme for Global Error. Here, we introduce some notations to write DOPRI5 scheme in a more compact way. Instead of the identity matrices we will use I and for the vector in \mathbf{R}^s with all components equal to one will be denoted by e . Also \otimes which is known as Kronecker product will be used for the notations such as $e = e \otimes I_{2(N+1)}$. With these notations, DOPRI5 scheme can be written as

$$\tilde{w}_{n+1} = \tilde{w}_n + \Delta t_n \Phi^T F(t_n, y_n), \tag{3.6}$$

$$y_n = e\tilde{w}_n + \Delta t_n \Psi F(t_n, y_n), \tag{3.7}$$

where $y_n = (y_1^{(n)}, y_2^{(n)}, \dots, y_s^{(n)})^T \in \mathbf{R}^{s(2(N+1))}$.

In this more compact way to represent the DOPRI5 scheme, we introduce some notations. I_s represents an identity matrix with the size $s \times s$. The vector e stands for the vector in \mathbf{R}^s with all components are one. We put $\Psi = \Psi \otimes I_{2(N+1)}$, $\Phi = \Phi \otimes I_{2(N+1)}$, $e = e \otimes I_{2(N+1)}$ and $\mathbf{I} = I_s \otimes I_{2(N+1)}$ where Ψ is the $s \times s$ matrix with entries ψ_{ij} , $\Phi^T = (\phi_1, \phi_2, \dots, \phi_s)^T$ where \otimes is the Kronocker product. Let $Y_n = (Y_1^{(n)}, Y_2^{(n)}, \dots, Y_s^{(n)})^T \in \mathbf{R}^{s(2(N+1))}$ where $Y_i^{(n)} = \tilde{W}(t_n + c_i \Delta t_n)$ with \tilde{W} is the solution of Eq. (2.18) we define residual errors $\rho_n \in \mathbf{R}^{s(2(N+1))}$ and $r_n = (r_1^{(n)}, r_2^{(n)}, \dots, r_s^{(n)})^T \in \mathbf{R}^{s(2(N+1))}$ such that

$$\tilde{W}(t_{n+1}) = \tilde{W}(t_n) + \Delta t_n \Phi^T F(t_n, Y_n) + \rho_n, \tag{3.8}$$

$$Y_n = e\tilde{W}(t_n) + \Delta t_n \Psi F(t_n, Y_n) + r_n, \tag{3.9}$$

Considering the following order conditions of Runge-Kutta method given in [4], for any given $p, q \in \mathbf{N}$

$$\Phi^T c^{j-1} = \frac{1}{j}, \quad j \in [1, p], \tag{3.10}$$

$$\Psi c^{j-1} = \frac{1}{j} c^j, \quad j \in [1, q]. \tag{3.11}$$

We can define the vector $k = (k_1, k_2, \dots, k_s)^T$ by

$$k = \frac{1}{q!} \left(\frac{1}{q+1} c^{q+1} - \Psi c^q \right). \tag{3.12}$$

Expanding the Taylor series for Eqs. (3.8)-(3.9) we can write the followings

$$\rho_n = \Delta t_n^{p+1} \frac{1}{p!} \left(\frac{1}{p+1} - \Phi^T \Delta t_n^p \right) \tilde{W}^{p+1}(t_n) + \mathcal{O}(\Delta t_n^{p+2}), \tag{3.13}$$

$$r_i^{(n)} = \Delta t_n^{q+1} k_i \tilde{W}^{q+1}(t_n) + \mathcal{O}(\Delta t_n^{q+2}). \tag{3.14}$$



Substraction of Eqs. (3.6)-(3.7) from Eqs. (3.8)-(3.9) we can define the errors $\varepsilon_n = W(t_n) - \tilde{w}_n$ where $\xi_n = (\xi_1^n, \xi_2^n, \dots, \xi_s^n)^T = Y_n - y_n$ such that

$$\varepsilon_{n+1} = \varepsilon_n + \Phi^T \mathbf{Z}_n \xi_n + \rho_n, \quad (3.15)$$

$$\xi_n = \mathbf{e} \varepsilon_n + \Psi \mathbf{Z}_n \xi_N + r_n, \quad (3.16)$$

where $\mathbf{Z}_n \in L(\mathbf{R}^{s(2(N+1))})$ is the block diagonal matrix defined by as follows,

$$\mathbf{Z}_i^{(n)} = \Delta t_n \int_0^1 \tilde{f}'(t_n + c_i \Delta t_n, y_i^{(n)} + \theta(Y_i^{(n)} - y_i^{(n)})) d\theta, \quad 1 \leq i \leq s, \quad (3.17)$$

with $\tilde{f}'(t, \tilde{w})$ is the Jacobian matrix $\frac{\partial \tilde{f}(t, \tilde{w})}{\partial \tilde{w}}$. By using the same approach to [4], the following result is obtained

$$\varepsilon_{n+1} = [\mathbf{I} + \Phi^T \mathbf{Z}_n (\mathbf{I} - \Psi \mathbf{Z}_n)^{-1} \mathbf{e}] \varepsilon_n + \Phi^T \mathbf{Z}_n (\mathbf{I} - \Psi \mathbf{Z}_n)^{-1} r_n + \rho_n. \quad (3.18)$$

In the light of all the results obtained, the convergence analysis of the adaptive Runge-Kutta method is completed with the theorem given below. For a detailed proof of the theorem, see [4].

Theorem 3.1. *Assume that the adaptive Runge-Kutta method defined in Eqs. (2.20)-(2.22) is A-stable with the stability function defined by $R(z) = 1 + \Phi^T z (\mathbf{I} - \Psi z)^{-1} \mathbf{e}$, such that $|R(z)| \leq 1$ for all $z \in \mathbf{C}^-$ then we have the following convergence result for $p = s - 1$,*

$$\|\varepsilon_n\| \leq C \Delta t_n^p. \quad (3.19)$$

Proof. For the proof of the Theorem 3.1, the referenced article can be examined. The conclusion was reached by considering the path followed in the reference article in [4]. In order to show the error bound given in Eq. (3.19), we use the perturbed error scheme which is defined in Eq. (3.18) which can be obtained for the given vectors $v_n \in \mathbf{R}^{2(N+1)}$ and $w_n \in \mathbf{R}^{2(N+1)}$ we can define,

$$\tilde{\varepsilon}_n = \varepsilon_n + v_n, \quad (3.20)$$

$$\tilde{\xi}_n = \xi_n + (\mathbf{I} - \Psi \mathbf{Z}_n)^{-1} w_n. \quad (3.21)$$

Inserting this into Eqs. (3.15) and (3.16) we arrive

$$\tilde{\varepsilon}_{n+1} = [\mathbf{I} + \Phi^T \mathbf{Z}_n (\mathbf{I} - \Psi \mathbf{Z}_n)^{-1}] \tilde{\varepsilon}_n + \Phi^T \mathbf{Z}_n (\mathbf{I} - \Psi \mathbf{Z}_n)^{-1} \tilde{r}_n + \tilde{\rho}_n, \quad (3.22)$$

where

$$\tilde{\rho}_n = \rho_n + v_{n+1} - v_n - \Phi^T \mathbf{Z}_n (\mathbf{I} - \Psi \mathbf{Z}_n)^{-1} w_n, \quad (3.23)$$

$$\tilde{r}_n = r_n - \mathbf{e} v_n + w_n. \quad (3.24)$$

In this perturbed error scheme with $v_n = \tau^{s-1} W^{(s-1)}(t_n)$ and $w_n = \mathbf{e} v_n - \mathbf{k} \tau^{s-1} W^{(s-1)}(t_n)$ where $\mathbf{k} = k \otimes I_{2(N+1)}$ we have,

$$\tilde{r}_n = r_n - \mathbf{k} \tau^{s-1} W^{(s-1)}(t_n), \quad (3.25)$$

$$\tilde{\rho}_n = \Phi^T \mathbf{Z}_n (\mathbf{I} - \Psi \mathbf{Z}_n)^{-1} [\mathbf{k} - \mathbf{e}] \tau^{s-1} W^{(s-1)}(t_n) + \tau^{s-1} [W^{(s-1)}(t_{n+1}) - W^{(s-1)}(t_n)] + \rho_n, \quad (3.26)$$

which satisfies the inequalities $\|\tilde{r}_n\| \leq C_1 \tau^s$ and $|\tilde{\rho}_n| < C_2 \tau^s$. Hence we get the result

$$\|\tilde{\varepsilon}_N\| \leq C \tau^{s-1}, \quad (3.27)$$

for certain C , $\tau > 0$ and since

$$\|\tilde{\varepsilon}_N - \varepsilon_N\| \leq \gamma \tau^{s-1} |W^{(s-1)}(t_n)|, \quad (3.28)$$

the order $s - 1$ result follows. \square



4. NUMERICAL RESULTS

Here, we consider the coupled Burger’s equations introduced by Esipov [7], with different initial and boundary conditions. The numerical solutions derived by the quintic B-spline method with adaptive time are exhibited for the various test examples examined in [16]. Different cases are studied with the various parameters and the accuracy of the presented method is investigated to several test problems which are considered in literature.

The accuracy of the method is measured using the following L_2 and L_∞ norms:

$$L_2(u) = \sqrt{\frac{\sum_{j=0}^N \|u_{exact}(x_j,t) - u_{approx}(x_j,t)\|^2}{\sum_{j=0}^N \|u_{exact}(x_j,t)\|^2}}, \tag{4.1}$$

$$L_\infty(u) = \max_{0 \leq j \leq N} \|u_{exact}(x_j,t) - u_{approx}(x_j,t)\|, \tag{4.2}$$

where x_j denotes the uniform knot sequences such that $x_j = jh$ with $h = \frac{b-a}{N}$ where $j = 0, 1, \dots, N$.

Example 4.1. As a first test problem we consider the Eqs. (1.1)-(1.2) for the coefficients $p = q = 1$ and $\eta = \xi = -2$ and $N = 50$ with following initial and boundary conditions [16],

$$u(x, 0) = v(x, 0) = \sin(x), \quad -\pi \leq x \leq \pi, \tag{4.3}$$

and

$$u(-\pi, t) = u(\pi, t) = 0, \quad 0 \leq t \leq T, \tag{4.4}$$

$$v(-\pi, t) = v(\pi, t) = 0, \quad 0 \leq t \leq T. \tag{4.5}$$

The exact solution of the Eqs. (1.1)-(1.2) is as follows which is described in [10]

$$u(x, t) = v(x, t) = e^{-t} \sin(x). \tag{4.6}$$

TABLE 3. Absolute maximum error values of first example, Example 4.1

t	[15]	[16]	QBS-DOPRI5	QBS-DOPRI5
	$L_\infty(u) = L_\infty(v)$	$L_\infty(u) = L_\infty(v)$	$L_\infty(u) = L_\infty(v)$	$L_2(u) = L_2(v)$
0.5	1.51688e-04	1.103080984e-04	1.97987e-07	7.89980e-07
1.0	1.83970e-04	1.336880384e-04	2.65422e-07	1.07654e-06
2.0	1.35250e-04	9.818252567e-05	2.43943e-07	1.05266e-06
3.0	7.46014e-05	1.029870405e-05	1.86235e-07	8.68148e-07

TABLE 4. The absolute maximum error values of first example, Example 4.1, at final time $t = 1$ with various time steps

Δt	[15]	[16]	QBS-DOPRI5	QBS-DOPRI5
	$L_\infty(u) = L_\infty(v)$	$L_\infty(u) = L_\infty(v)$	$L_\infty(u) = L_\infty(v)$	$L_2(u) = L_2(v)$
0.02	3.70976e-03	1.336881168e-03	3.46659e-07	1.51329e-06
0.01	1.84705e-03	1.336880384e-04	2.65422e-07	1.07654e-06
0.005	9.21572e-04	1.336871098e-04	2.80220e-07	1.15089e-06
0.002	4.60280e-04	1.336581399e-04	2.49910e-07	9.78322e-07
0.001	1.83970e-04	1.335581399e-04	3.62781e-07	1.601140e-07



In the first computation, the maximum errors are presented at various time levels and corresponding results are given in Table 3. Compared to other studies in literature, it is clear that our presented method gives better results. In Table 4, the absolute maximum error results are computed with different Δt time steps at final time of $t = 1$ for the same coefficients.

As can be seen in the presented figures the results are the same for $u(x, t)$ and $v(x, t)$ solutions because of the symmetry at initial and boundary conditions. Corresponding illustrations are displayed in Figure 1 and 2.

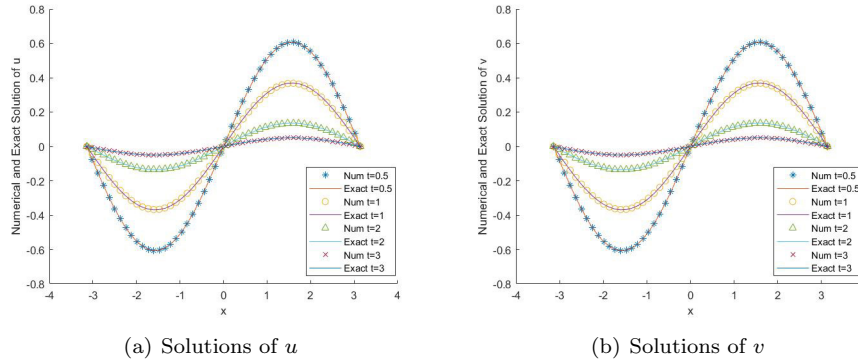


FIGURE 1. The graphics of numerical solutions of first example, Example 4.1, at different final times

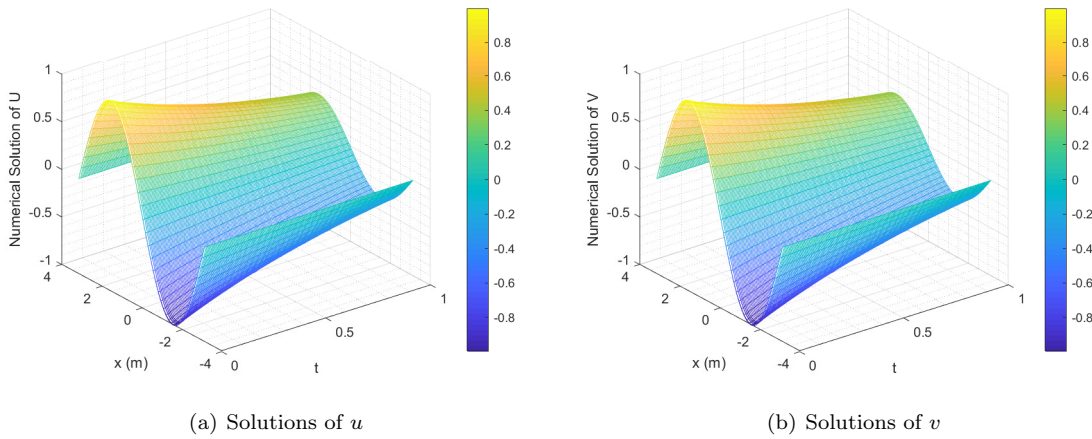


FIGURE 2. The graphics of numerical solutions of first example, Example 4.1

Example 4.2. In this example, we solve the Eqs. (1.1)-(1.2) for $\eta = \xi = 2$ with different values of p and q at various final times for $N = 50$. The exact solutions of the problem which are given in [15] as follows,

$$u(x, t) = a_0 - 2A \left(\frac{2p - 1}{4pq - 1} \right) \tanh(A(x - 2At)), \quad -10 \leq x \leq 10, \quad t > 0, \tag{4.7}$$

$$v(x, t) = a_0 \left(\frac{2q - 1}{2p - 1} \right) - 2A \left(\frac{2p - 1}{4pq - 1} \right) \tanh(A(x - 2At)), \quad -10 \leq x \leq 10, \quad t > 0, \tag{4.8}$$

where $a_0 = 0.05$ and $A = \frac{a_0(4pq - 1)}{4p - 2}$. The initial and boundary conditions are taken from the exact solutions.



TABLE 5. Absolute maximum error values of $u(x, t)$ for second example, Example 4.2, with $\Delta t = 0.01$

t	p	q	[15]	[19]	[11]	QBS-DOPRI5
0.5	0.1	0.3	1.44e-003	9.619e-004	4.173e-005	4.2600e-05
	0.3	0.03	6.68e-004	4.310e-004	4.585e-005	4.5880e-05
1.0	0.1	0.3	1.27e-003	1.153e-003	8.275e-005	8.2805e-05
	0.3	0.03	1.30e-003	1.268e-003	9.167e-005	9.1799e-05
3.0	0.1	0.03	2.408e-004	2.3930e-04
	0.1	0.03	2.747e-004	2.5185e-04

The numerical solutions have been obtained for the domain $x \in [-10, 10]$ with $\Delta t = 0.01$. Table 5 and 6 exhibit the comparison of the maximum errors proposed method with the literature. Although the proposed method has similar results given in [11] it is observed that it gives quite good results when we compare it with other methods.

TABLE 6. Absolute maximum error values of $v(x, t)$ for second example, Example 4.2, with $\Delta t = 0.01$

t	p	q	[15]	[19]	[11]	QBS-DOPRI5
0.5	0.1	0.3	5.42e-004	3.332e-004	5.418e-005	2.2171e-05
	0.3	0.03	1.20e-003	1.148e-003	2.826e-005	1.8088e-04
1.0	0.1	0.3	1.29e-003	1.162e-003	1.074e-004	4.1027e-05
	0.3	0.03	2.35e-003	1.638e-003	5.673e-005	3.6100e-04
3.0	0.1	0.03	3.119e-004	1.1405e-04
	0.1	0.03	1.663e-004	2.9210e-04

Example 4.3. Now, we consider the coupled Burger’s equations (1.1)-(1.2) with the following initial and zero boundary conditions.

$$u(x, 0) = \begin{cases} \sin(2\pi x), & 0 \leq x \leq 0.5, \\ 0, & 0.5 < x \leq 1, \end{cases}$$

$$v(x, 0) = \begin{cases} 0, & 0 \leq x \leq 0.5, \\ -\sin(2\pi x), & 0.5 < x \leq 1. \end{cases}$$

TABLE 7. Numerical solution values $u(x, t)$ for third examples, Example 4.3, at different final times

Maximum value of u for $p = q = 10$						
t	[16]	[14]	QBS-DOPRI5	At point	CPU Time	
0.1	0.144491495800	0.14456	0.14452	0.58	0.80	
0.2	0.052356151890	0.05237	0.05238	0.54	1.32	
0.3	0.019318838080	0.01932	0.01933	0.52	2.16	
0.4	0.007184856672	0.00718	0.00719	0.50	2.98	

The numerical solutions of Example 4.3 are obtained for $x \in [0, 1]$ and the results are given for different coefficients of p and q . In Table 7, the coefficients p and q are taken 10 with $\eta = \xi = 2$ and the maximum solution values of u are given at different final times. The maximum solution values of v for $p = q = 100$ with $\eta = \xi = 2$ are exhibited at different final times in Table 8. It is observed that the computed results are in a good agreement with the literature and according to the observed CPU times in Tables 7 and 8 the numerical solutions can be computed in less than 4 second CPU times. Also corresponding solutions are shown in Figure 3 for $t = 0.0001, 0.001, 0.01$ and 0.1 . We also note that as the values of convection parameters are enhanced, the numerical solutions approach to zero. It is exhibited in Figures 4 and 5 .



TABLE 8. Numerical solution values $v(x, t)$ for third examples, Example 4.3, at different final times

Maximum value of v for $p = q = 100$					
t	[16]	[14]	QBS-DOPRI5	At point	CPU Time
0.1	0.050737669860	0.05065	0.05080	0.76	0.80
0.2	0.010356602970	0.01033	0.01036	0.64	1.55
0.3	0.003517189432	0.00350	0.00351	0.56	2.16
0.4	0.001294450199	0.00129	0.00129	0.52	3.64

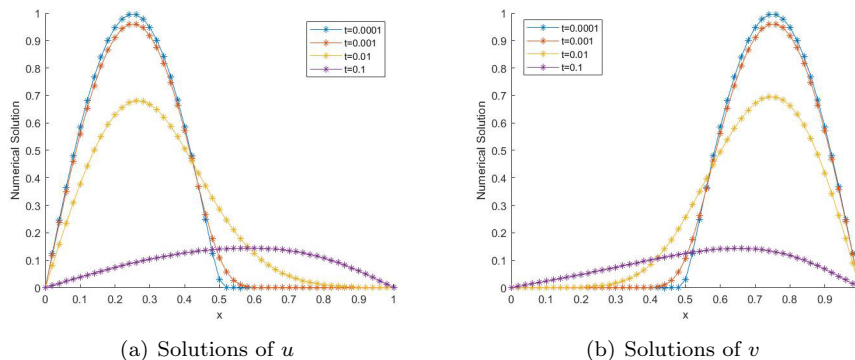


FIGURE 3. The graphics of numerical solutions of third example, Example 4.3, at different final times

5. CONCLUSION

In this work, an effective method of line approach is applied to the coupled Burger’s equation. To approximate the spatial derivatives, quintic B-spline functions are used. The resulting system of ordinary differential equations, gained using this approximation, is solved with an adaptive time integration scheme called DOPRI5. Compared to other methods, the proposed method of applying the higher-order scheme for time has enabled us to obtain more accurate solutions in a shorter time. The convergence analysis has been studied in the derivation of the proposed method’s uniform global error bounds. In addition to these theoretical results, the current study has also been enhanced computationally by applying the proposed method to the coupled Burger’s equation for different initial and boundary values. The first two examples have analytical solutions. It can be seen from the tables and simulations that the proposed method for these examples has better accuracy than the given studies in the literature. In the third example, it is seen that computed solutions are in good agreement with the numerical solutions in literature and solutions can be obtained in less than four seconds CPU times, which is a very short time. As a result, the proposed method is a practical and convenient approach for solving a wide range of partial differential equations.



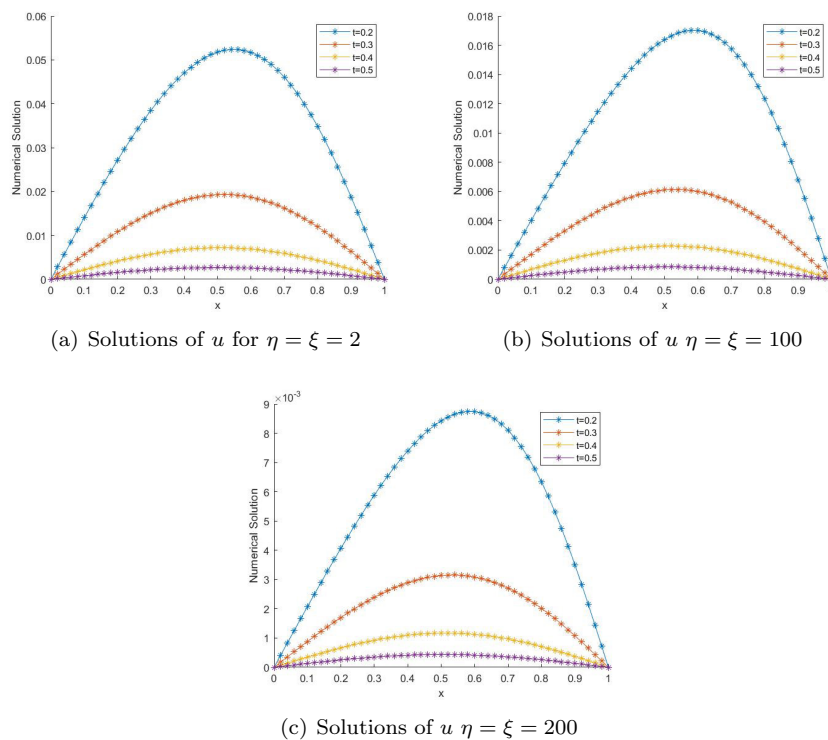


FIGURE 4. The graphics of numerical solutions of Example 4.3, with enhancing values of convection coefficients at different final times

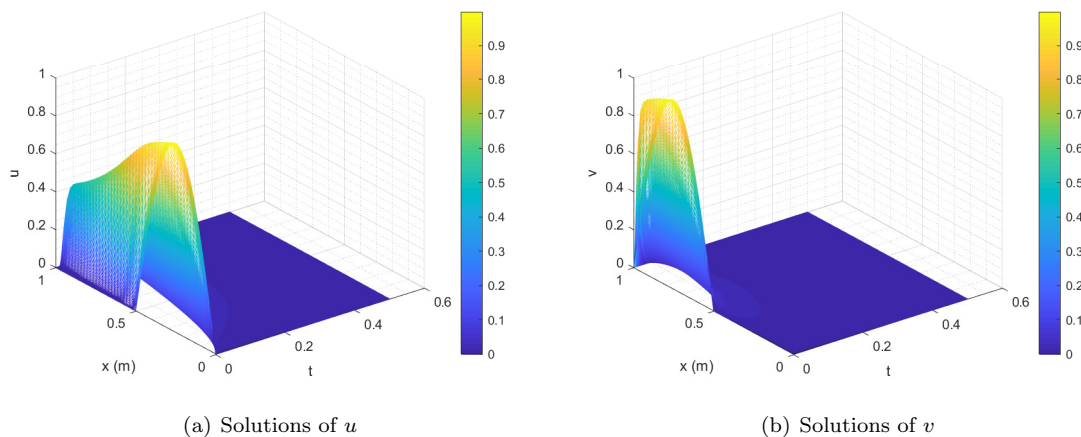


FIGURE 5. The graphics of numerical solutions of first example, Example 4.3

REFERENCES

- [1] H. Ahmad, T. A. Khan, and C. Cesarano, *Numerical solutions of coupled Burger's equations*, *Axioms*, 8(4) (2019), 119.
- [2] E. Bahar and G. Gurarlan, *B-spline method of lines for simulation of contaminant transport in groundwater*, *Water*, 12(1607) (2020), 1–21.
- [3] S. Bak, P. Kim, and D. Kim, *A semi-lagrangian approach for numerical simulation of coupled Burgers' equations*, *Commun. Nonlinear Sci. Numer. Simulation*, 69 (2019), 31–44.
- [4] K. Burrage, W. H. Hunndsdorfer, and J. G. Verwer, *A study of b-convergence of runge-kutta methods*, *Computing*, 36 (1986), 17–34.
- [5] J. C. Butcher, *Implicit runge-kutta processes*, *Mathematics of Computation*, 18(85) (1964), 50–64.
- [6] J. R. Dormand and P. J. Prince, *A family of embedded runge-kutta formulae*, *Journal of Computation and Applied Mathematics*, 6(1) (1980), 19–26.
- [7] S. E. Esipov, *Coupled burgers equations: A model of polydispersive sedimentation*, *Phys Rev E Stat Phys Plasmas Fluids Relat Interdiscip Topics*, 52(4) (1995), 3711–3718.
- [8] D. Irk, I. Dag, and M. Tombul, *Extended cubic b-spline solution of the advection-diffusion equation*, *KSCE J. Civ. Eng.*, 19(4) (2014), 929–934.
- [9] S. U. Islam, S. Haq, and M. Uddin, *A meshfree interpolation method for the numerical solution of the coupled nonlinear partial differential equations*, *Eng. Anal. Bound. Elem.*, 33(3) (2009), 399–409.
- [10] D. Kaya, *An explicit solution of coupled viscous burgers' equation by the decomposition method*, *Int. J. Math. and Math. Sci.*, 27(11) (2001), 675–680.
- [11] A. H. Khater, R. S. Temsah, and M. M. Hassan, *A chebyshev spectral collocation method for solving Burgers'-type equations*, *J. Comput. Appl. Math.*, 222(2), 333–350.
- [12] A. Korkmaz and I. Dag, *Quartic and quintic b-spline methods for advection–diffusion equation*, *Appl. Math. Comput.*, 274(1) (2016), 208–219.
- [13] M. Kumar and S. Pandit, *A composite numerical scheme for the numerical simulation of coupled Burgers' equation*, *Comput. Phys. Commun.*, 185(3) (2014), 809–817.
- [14] R. C. Mittal and G. Arora, *Numerical solution of the coupled viscous Burgers' equation*, *Commun. Nonlinear Sci. Numer. Simul.*, 16(3) (2011), 1304–1313.
- [15] R. C. Mittal and R. Jiwari, *Differential quadrature method for numerical solution of coupled viscous Burgers equations*, *Int. Journal for Comp. Methods in Eng. Science and Mechanics*, 13(2) (2012), 88–92.
- [16] R. C. Mittal and A. Tripathi, *A collocation method for numerical solutions of coupled Burgers' equations*, *Int. Journal for Comp. Methods in Eng. Science and Mechanics*, 15(5) (2014), 457–471.
- [17] T. Nazir, M. Abbas, A. I. M. Ismail, A. A. Majid, and A. Rashid, *The numerical solution of advection—diffusion problems using new cubic trigonometric b-splines approach*, *Appl. Math. Model.*, 40(7-8) (2016), 4586–4611.
- [18] K. R. Raslan, T. E. Danaf, and K. K. Ali, *Collocation method with quintic b-spline method for solving coupled Burger's equations*, *Fast East Jour. of App. Math.*, 96(1) (2017), 55–75.
- [19] A. Rashid and A. I. B. M. Ismail, *A fourier pseudospectral method for solving coupled viscous Burgers equations*, *Comput. Methods in Appl. Math.*, 9(4) (2009), 412–420.
- [20] A. Rashid, M. Abbas, A. I. M. Ismail, and A. A. Majid, *Numerical solution of the coupled viscous Burgers equations by chebyshev legendre pseudo-spectral method*, *Appl. Math. Comput.*, 245 (2014), 372–381.
- [21] Y. Zhang, J. Lin, S. Reutskiy, H. Sun, and W. Feng, *The improved backward substitution method for the simulation of time-dependent nonlinear coupled Burgers' equation*, *Results in Physics*, 18 (2020), 103231.

